Supplement of Atmos. Chem. Phys., 22, 16091–16109, 2022
https://doi.org/10.5194/acp-22-16091-2022-supplement

Supplement of

An evaluation of biomass burning aerosol mass, extinction, and size distribution in GEOS using observations from CAMP^{2}Ex

Allison B. Marquardt Collow et al.

Correspondence to: Allison B. Marquardt Collow (allison.collow@nasa.gov)

1. Figures

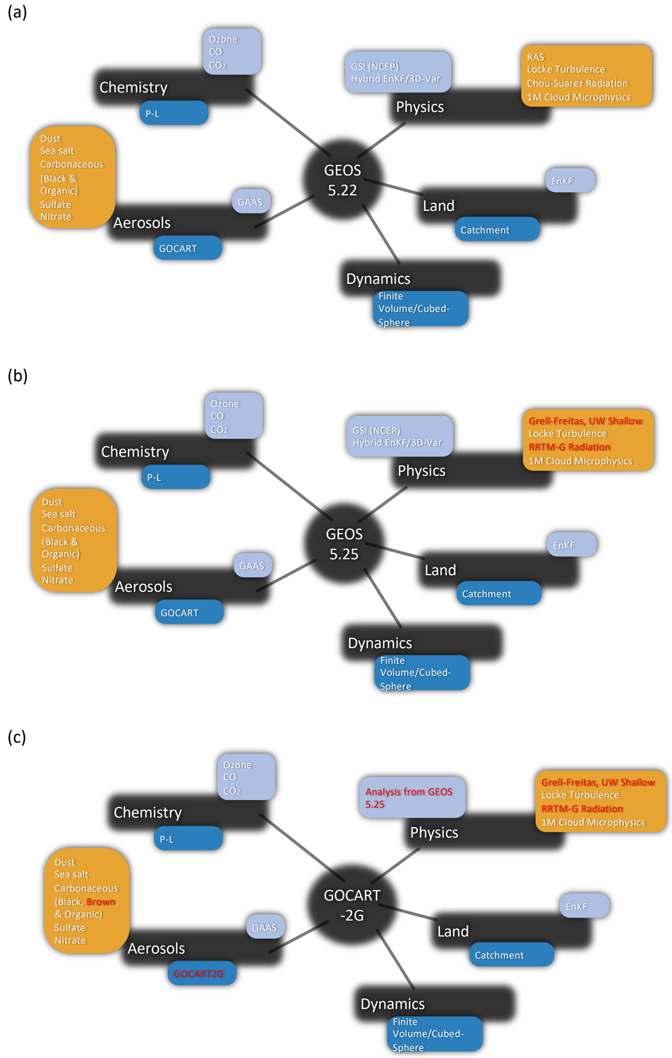

Figure S1. Modules incorporated in the (a) GEOS 5.22, (b) GEOS 5.25, and (c) GOCART2G simulations. Features highlighted in red indicate a change from the GEOS 5.22 baseline.

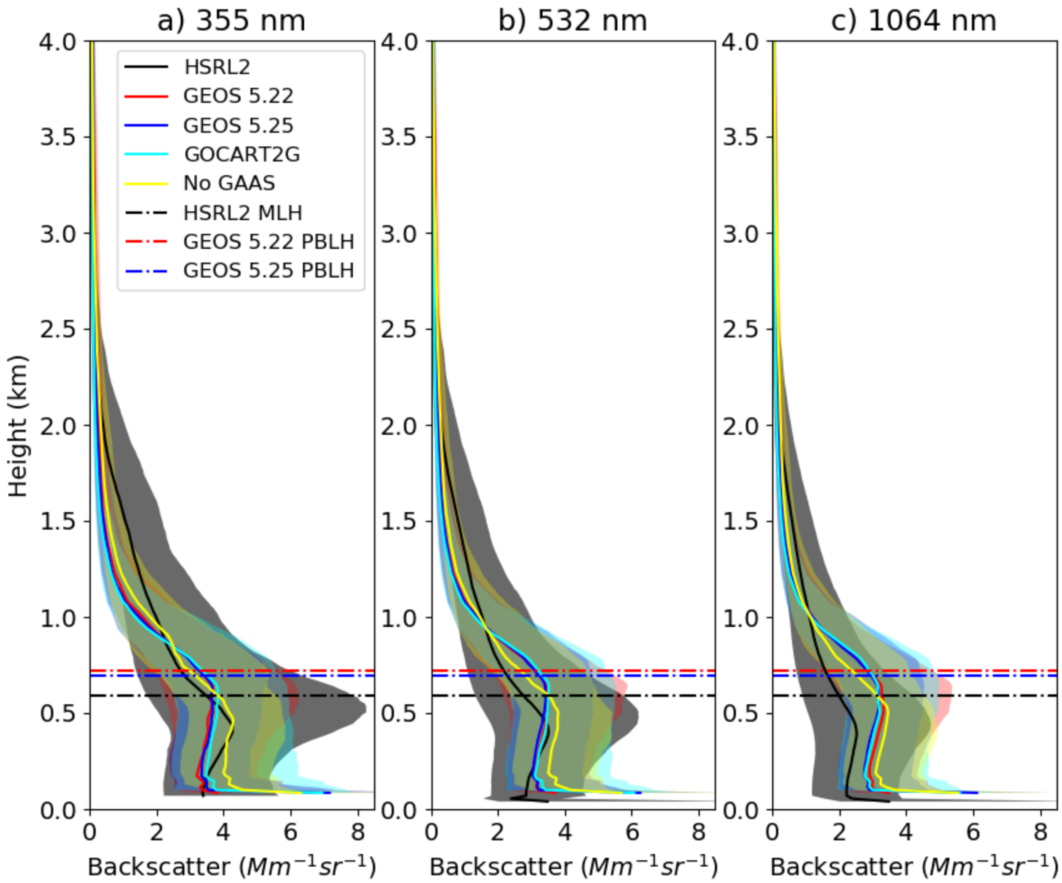

Figure S2: Median backscatter at (a) 355 nm, (b) 532nm, and 1064 nm during all research flights from the HSRL2, GEOS 5.22, GEOS 5.25, GOCART2G, and GOCART2G without aerosol assimilation (No GAAS). Profiles are shaded between the 25th and 75th percentiles. Mixed layer height (MLH) from the HSRL2 and planetary boundary layer (PBL) height in GEOS are added for reference as dashed lines. Note that PBL height for GOCART2G is the same as GEOS 5.25.

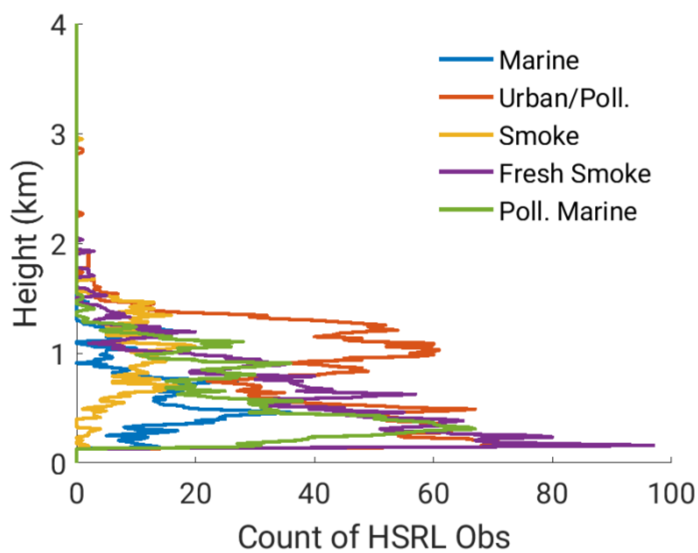

Figure S3: Vertical profile of the count of observations from the HSRL2 for each aerosol type

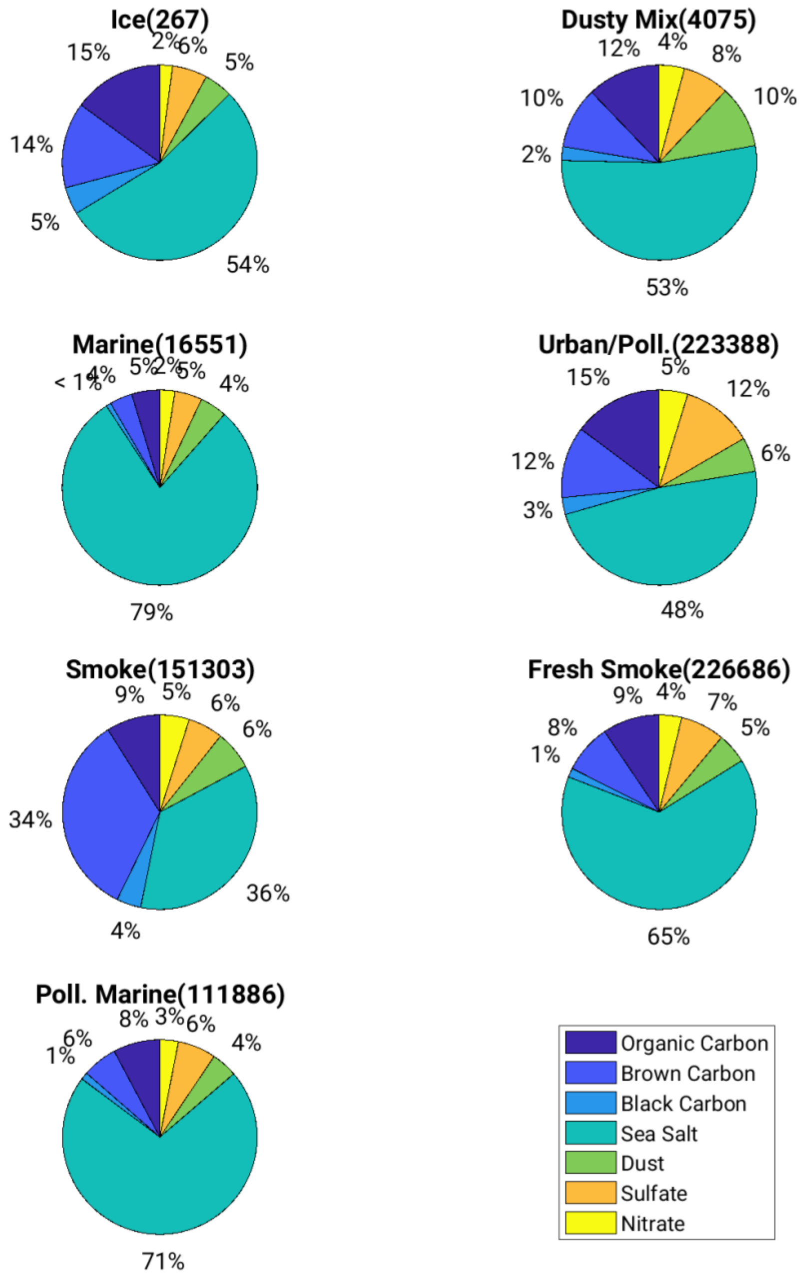

Figure S4: The aerosol speciation in GEOS GOCART2G composited based on the aerosol ID provided by the HSRL2. The values in parentheses indicate the total number of data points with each aerosol type.

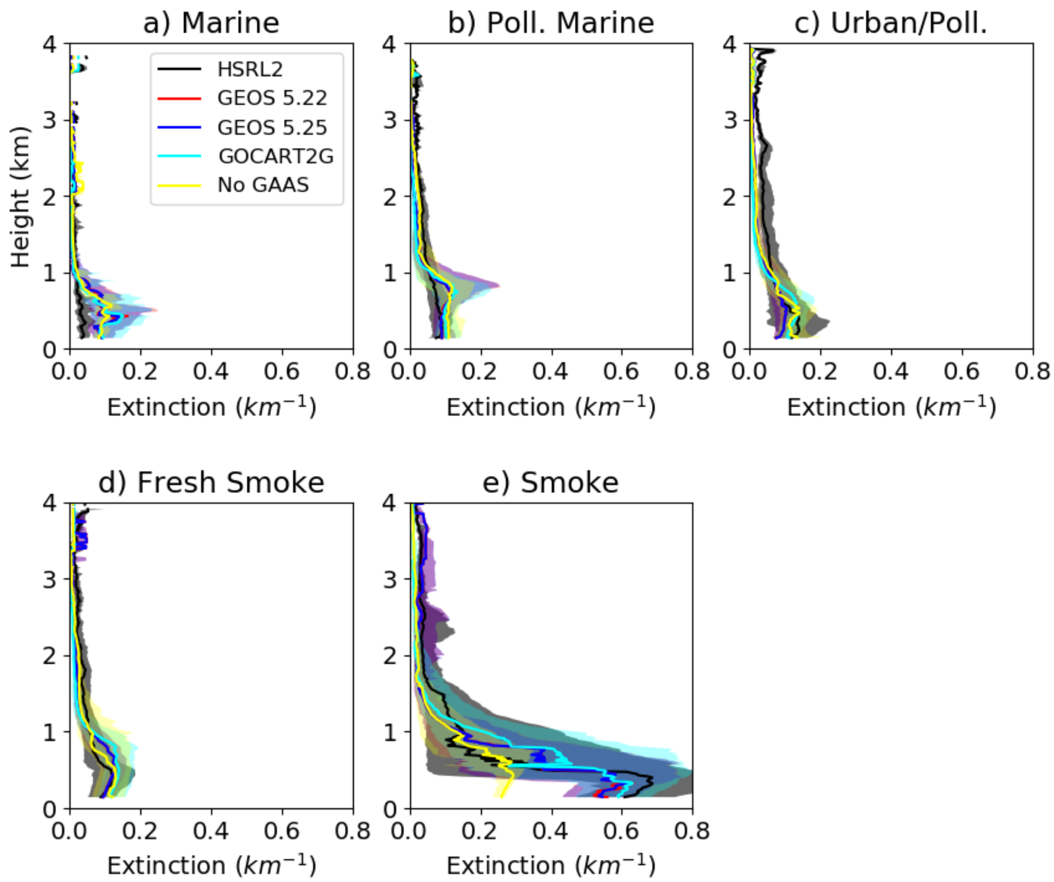

Figure S5. Median extinction at 532 nm during all research flights from the HSRL2, GEOS 5.22, GEOS 5.25, GOCART2G, and GOCART2G without aerosol assimilation (No GAAS) filtered based on the HSRL2 aerosol id for (a) marine, (b) polluted marine, (c) smoke, (d) fresh smoke, and (e) urban aerosols. Profiles are shaded between the 25th and 75th percentiles.

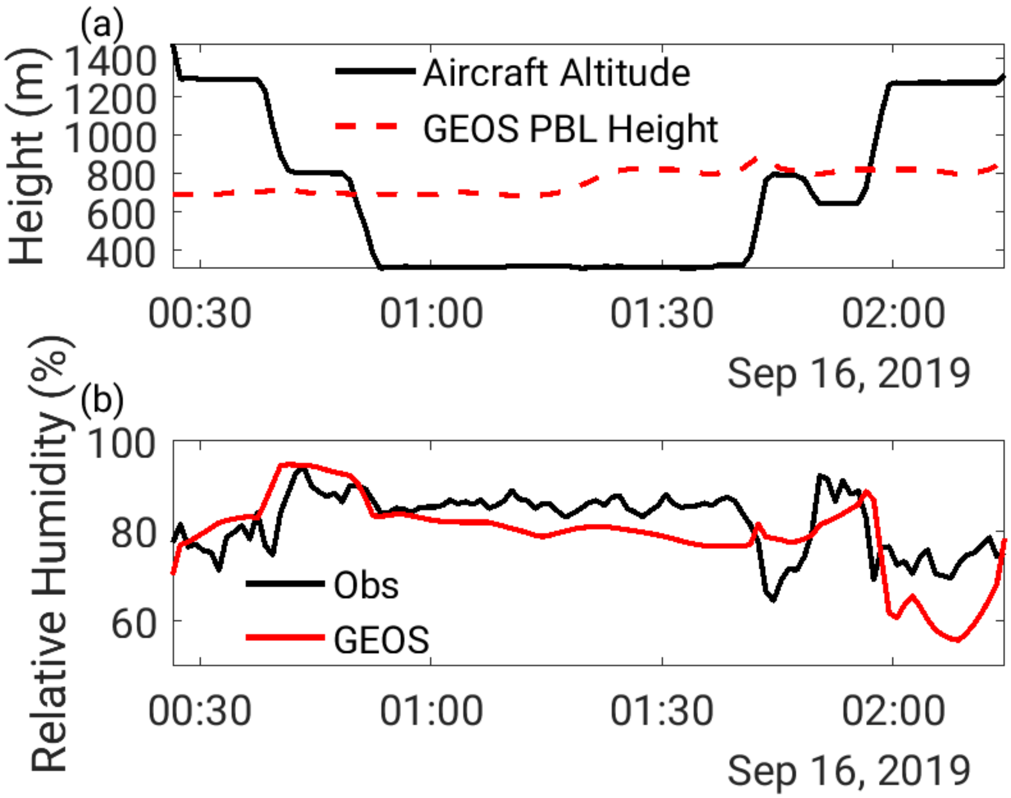

Figure S6: (a) Height of the aircraft during the smoke transect from RF9 in comparison to the height of the planetary boundary layer in GEOS and (b) the relative humidity from the observations and GEOS during the transect.

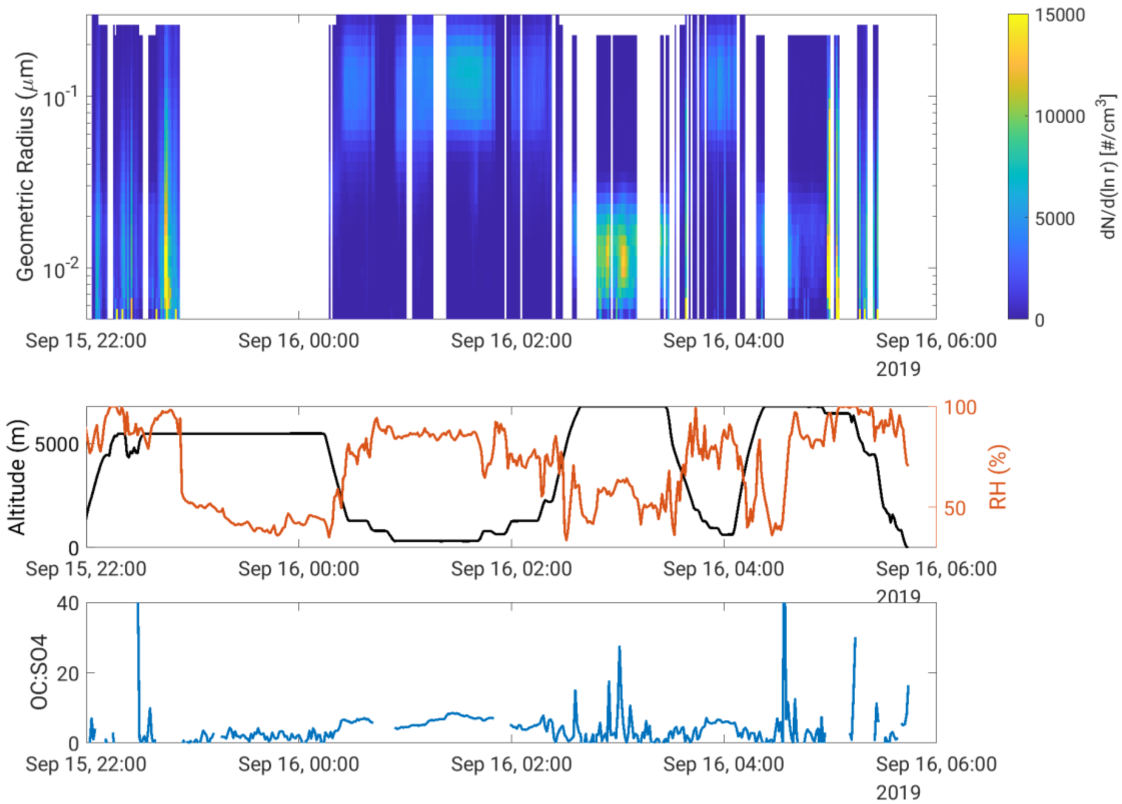

Figure S7: Timeseries of particle size distribution, aircraft altitude, relative humidity, and the ratio of organic carbon to sulphate during RF9.

2. Tables

Table S1. The radii and densities of the five size bins for dust used for settling in GEOS.

	DU001	DU002	DU003	DU004	DU005
Radius (μm)	0.73	1.4	2.4	4.5	8
Radius Lower Bound (μm)	0.1	1	1.8	3	6
Radius Upper Bound (μm)	1	1.8	3	6	10
Density (kg m^{-3})	2500	2650	2650	2650	2650

Table S2. The radii and densities of the five size bins for sea salt used for settling in GEOS

	SS001	SS002	SS003	SS004	SS005
Radius (μm)	0.079	0.316	1.119	2.818	7.772

Radius Lower Bound (µm)	0.03	0.1	0.5	1.5	5
Radius Upper Bound (µm)	0.1	0.5	1.5	5	10
Density (kg m^{-3})	2200	2200	2200	2200	2200

Table S3. The radii and densities used for the settling of nitrate and ammonium in GEOS. Note that NI002 and NI003 represent coarse mode nitrate formed from the heterogenous production of nitrate from sea salt and dust, respectively.

	NH_4^+	NI001	NI002	NI003
Radius (µm)	0.2695	0.2695	2.1	7.57
Density (kg m^{-3})	1769	1725	2200	2650

Table S4. File versions for the optics look up tables used for GOCART2G. These files are available for download at https://portal.nccs.nasa.gov/datashare/iesa/aerosol/AerosolOptics/.

Aerosol Species	Optics File
Black Carbon	opticsBands_BC.v1_3.RRTMG.nc
Brown Carbon	opticsBands_BRC.v1_5.RRTMG.nc
Organic Carbon	opticsBands_OC.v1_3.RRTMG.nc
Dust	opticsBands_DU.v15_3.RRTMG.nc
Sea Salt	opticsBands_SS.v3_3.RRTMG.nc
Nitrate	opticsBands_NI.v2_5.RRTMG.nc
Sulfate	opticsBands_SU.v1_3.RRTMG.nc

3. Supporting Information for the Schill Particle Size Distribution

Merging the Particle Analysis by Laser Mass Spectrometry (PALMS) number fractions with an independently measured, quantitative size distribution to make species-specific (e.g., biomass burning, dust, sea salt) size distributions has been detailed in several publications (e.g., Froyd et al., 2019; Brock et al., 2021). The biomass-burning-only size distributions from the Studies of Emissions and Atmospheric Composition, Clouds and Climate Coupling by Regional Surveys (Toon et al., 2016) and NASA Atmospheric Tomography (Thompson et al., 2022) missions are used. Using both missions allows us to assess the biomass-burning-only size distributions from plumes <1 day old to biomass burning aerosol that have aged in the atmosphere ~30 days. We find that, regardless of age, the biomass burning size distribution can be described by a single lognormal mode. In this work, we use the size distributions from fires <5 days old. The rn, median and σ values from these size distributions are 0.1175 µm and 1.3, respectively (Schill et al., 2021).

4. References

Brock, C. A., Froyd, K. D., Dollner, M., Williamson, C. J., Schill, G., Murphy, D. M., . . . Wofsy, S. C. (2021). Ambient aerosol properties in the remote atmosphere from global-scale in situ measurements. Atmospheric Chemistry and Physics, 21 (19), 15023–15063. doi: 10.5194/acp-21-15023-2021.

Froyd, K. D., Murphy, D. M., Brock, C. A., Campuzano-Jost, P., Dibb, J. E., Jimenez, J.-L., . . . Ziemba, L. D. (2019). A new method to quantify mineral dust and other aerosol species from aircraft platforms using single-particle mass spectrometry. Atmospheric Measurement Techniques, 12 (11), 6209–6239. doi: 10.5194/amt-12-6209-2019.

Schill, G.P., et al, Size Distributions of Biomass Burning Aerosol as a Function of Age and Comparisons to Models, AAAR 39th Annual Meeting, Virtual, 18-22 October 2021, 12SW.4, 2021.

Thompson, C. R., Wofsy, S. C., Prather, M. J., Newman, P. A., Hanisco, T. F., Ryerson, T. B., . . . Zeng, L. (2022). The NASA Atmospheric Tomography (ATom) Mission: Imaging the Chemistry of the Global Atmosphere. Bulletin of the American Meteorological Society, 103 (3), E761–E790. doi: 10.1175/BAMS-D -20-0315.1.

Toon, O. B., Maring, H., Dibb, J., Ferrare, R., Jacob, D. J., Jensen, E. J., . . . Pszenny, A. (2016). Planning, implementation, and scientific goals of the Studies of Emissions and Atmospheric Composition, Clouds and Climate Coupling by Regional Surveys (SEAC 4 RS) field mission. Journal of Geophysical Research: Atmospheres, 121 (9), 4967–5009. doi: 10.1002/2015JD024297